CRISPR/Cas9-mediated claudin-2 knockout in HCT116 cells reveals its key role in colorectal cancer progression

RANA A. ALGHAMDI[1,2] and MARYAM H. AL-ZAHRANI[3]

[1]Department of Chemistry, Science and Arts College, King Abdulaziz University, Rabigh 21911, Saudi Arabia;
[2]Regenerative Medicine Unit, King Fahd Medical Research Center, King Abdulaziz University, Jeddah 80216, Saudi Arabia;
[3]Department of Biochemistry, Faculty of Science, King Abdulaziz University, Jeddah 21589, Saudi Arabia

Received July 28, 2025; Accepted October 31, 2025

DOI: 10.3892/ol.2025.15407

Abstract. Colorectal cancer (CRC) progression involves complex mechanisms of invasion and metastasis. Claudin-2 (*CLDN2*), a tight junction protein, has emerged as a key regulator paracellular permeability and its dysregulation is implicated in chronic inflammatory diseases and cancer. The present study aimed to determine the mechanisms by which *CLDN2* deletion affects genes associated with motility and invasion of colon cancer cells. CRISPR/Cas9 was used to knock out *CLDN2* in HCT116 cells. Subsequently, gene expression was analyzed using reverse transcription-quantitative PCR and migratory capacity was assessed using wound healing assays. *CLDN2* deletion led to the downregulation of genes associated with motility and metastasis, including zonula occludens-1-associated nucleic acid binding protein, N-Myc downstream-regulated gene 1, *CLDN14*, *CLDN23*, *Bcl-2*, *p53* and *Bcl-6*, suggesting that *CLDN2* supports pro-migratory gene networks. These findings demonstrated that *CLDN2* regulates metastatic gene expression in CRC. Although further mechanistic studies are warranted, the present study provided notable genetic and phenotypic evidence of the role of *CLDN2* in promoting cancer cell migration and invasion, offering a potential foundation for future studies into its signaling interactions and therapeutic potential.

Introduction

Colorectal cancer (CRC) is a major cause of cancer-associated mortality worldwide, In 2023, an estimated 1.97 million new cases of CRC and ~0.93 million deaths were reported globally (1). The burden of CRC is increasing in Eastern Asia, the Middle East, and parts of Southeast Asia, where rapid lifestyle transitions, Westernized diets, and limited early-screening coverage have contributed to rising incidence trends (2). In Asia, ~992,000 new CRC cases and ~498,000 related deaths were reported in 2020 (3). Proteomic and genomic studies have advanced cancer research by revealing molecular pathways involved in CRC particularly through dysregulated signaling cascades that drive tumor development and progression, such as the Wnt/β-catenin, PI3K/AKT signaling, MAPK/ERK pathway, and alterations in TP53-regulated stress response networks, all of which play key roles in cell proliferation, survival, and metastasis (4). Among key molecular players, claudin-2 (*CLDN2*), a component of tight junctions, has emerged as a contributor to malignancy by exhibiting aberrant expression (5).

The claudin family serves a key role in cell barriers, differentiation and proliferation. The expression patterns of claudin knockout (KO) vary throughout malignancies and organs (6). Thus, claudins have been proposed as targets for cancer treatment as well as diagnostic indicators. Previous research has demonstrated an increasing consensus on the potential value of *CLDN2* as a biomarker for prognostic and therapeutic features in CRC (7-9). Notably, *CLDN2* expression is elevated in inflammatory bowel disease and colorectal tumors compared with normal tissues (10).

CLDN2 has diverse biological functions beyond maintaining epithelial permeability. It contributes to paracellular water and ion transport, modulates epithelial proliferation and participates in signaling events associated with oncogenic transformation (8,11). Elevated *CLDN2* levels have been associated with poor prognosis, advanced tumor stages and increased metastatic potential in several cancer types, including CRC (7,12). These findings highlight the importance of understanding the multifunctional role of *CLDN2* in colorectal carcinogenesis. *CLDN2* is the most distinct member of the claudin family and exhibits a unique expression pattern because its expression is limited to permeable epithelial tissues (11). In colon cancer, *CLDN2* appears to function as an oncogene, enhancing cell proliferation and migration capacity through EGFR-mediated pathways (12). Notably, the increasing incidence of CRC has been connected to the presence of *CLDN2* in cellular tight junctions.

Correspondence to: Dr Rana A. Alghamdi, Department of Chemistry, Science and Arts College, King Abdulaziz University, Rabigh Campus, Faculty Building 4, King Abdulaziz Road, Rabigh 21911, Saudi Arabia
E-mail: raalghamdi3@kau.edu.sa

Key words: CRISPR/Cas9, claudin-2, colorectal cancer, tight junction protein, gene expression, knockout

Mechanistically, it has been demonstrated that *CLDN2* inhibits the transcription of N-Myc downstream-regulated gene 1 (NDRG1), a well-established metastasis suppressor gene. This repression is mediated through the recruitment of zonula occludens-1 (*ZO-1*)-associated nucleic acid binding protein (*ZONAB*) to the *NDRG1* promoter, where *CLDN2* facilitates *ZONAB* binding and suppresses *NDRG1* transcriptional activity (13).

Elevated *CLDN2* expression has been observed in CRC compared with adjacent normal tissue and is associated with shorter cancer-specific survival and increased risk of recurrence in stage II/III CRC receiving adjuvant therapy (14). Although environmental and genetic variables can affect CRC, such as diet, obesity, and smoking, understanding the mechanisms by which *CLDN2* functions during CRC development could help identify potential novel treatment options in the future. High *CLDN2* expression patterns reported shorter survival outcomes, indicating a connection between high *CLDN2* expression and CRC progression (13).

While genomic analyses have identified driver mutations in CRC, understanding the mechanisms by which specific proteins such as *CLDN2* integrate into oncogenic signaling networks remains challenging (15-17). CRISPR/Cas9-based gene editing offers a key tool to dissect functional roles by enabling precise gene KO models (18). Furthermore, combining CRISPR approaches with gene expression profiling allows for further investigation into CRC biology and the identification of potential novel therapeutic targets in the future (19). Due to the limited mechanistic understanding of *CLDN2* in CRC, the present study aimed to investigate the effects of *CLDN2* deletion on gene expression patterns associated with migration, invasion and metastasis. A CRISPR/Cas9-mediated KO approach was used in HCT116 cells to assess both phenotypic changes and transcriptional alterations, with a focus on pathways implicated in CRC progression.

Materials and methods

Cell culture. The human CRC cell line HCT116 (cat. no. CCL-247; American Type Culture Collection) was obtained from Synthego. The HCT116 cell line is a widely used model of CRC repair deficiency due to a mutation in the mutL homolog 1 gene. Cells were authenticated by short tandem repeat profiling, and were confirmed to be mycoplasma-free prior to use.

Wild-type (Wt) and *CLDN2*-KO HCT116 cells were cultured in McCoy's 5A medium (cat. no. 16600082; Thermo Fisher Scientific, Inc.) supplemented with 10% FBS (cat. no. 10270106; Thermo Fisher Scientific, Inc.) and 1% penicillin-streptomycin (cat. no. 15140-122; Thermo Fisher Scientific, Inc.). The cells were maintained at 37˚C in a humidified incubator with 5% CO_2.

Generation of CRISPR/Cas9-mediated CLDN2-KO cells. CRISPR/Cas9 mediated KO of human *CLDN2* (gene ID, 9075) in HCT116 cells was produced by Synthego. Guide RNA design and off-target prediction were performed using the Synthego CRISPR Design Tool (v1.2; Synthego). Ribonucleoprotein complexes consisting of Cas9 protein and a synthetic, chemically modified single-guide RNA (sgRNA) targeting exon 2 of human *CLDN2* (sgRNA sequence, 5'-GGU GCUAUAGAUGUCACACU-3') were electroporated into HCT116 cells. The sgRNA cut site was chrX:106,928,419. Following electroporation (20), single-cell clones were generated by fluorescence-activated cell sorting into 96- or 384-well plates and expanded (21). The assessment of editing efficiency was performed 48 h after electroporation. The process involved extracting genomic DNA (gDNA) from a subset of cells, followed by PCR amplification and sequencing using the Sanger sequencing method. Sequencing was performed in the forward direction using a 20-nt primer, generating 700-900 nt reads. Sanger sequencing services were provided by Synthego. PCR primers were as follows: Forward, 5'-CAGCCTGAA GACAAGGGAGC-3'; and reverse, 5'-TGTCTTTGGCTC GGGATTCC-3'. The sequencing primer used was as follows: 5'-CAGCCTGAAGACAAGGGAGC-3'. The chromatograms obtained were analyzed using the Synthego Inference of CRISPR edits (ICE; version 2.0 (Synthego) (22).

For insertion-deletion (indel), the indel examination was performed using the Illumina sequencing platform (Illumina, Inc.), according to the manufacturer's protocol (23). A total of 20 ng gDNA was utilized as a template for amplifying the region surrounding the sgRNA target site, using the specified primers. To generate monoclonal cell populations, cell pools with altered *CLDN2* gene (*CLDN2*-KO) were distributed at a density of 1 cell/well using a single cell printer onto either 96- or 384-well plates (24). Every 3 days, all wells were recorded to verify the growth of a clone originating from a single cell. The PCR-Sanger-ICE genotyping technique was used to screen and identify clonal populations.

Wound healing assay. The migratory capacity of Wt and *CLDN2*-KO cells was assessed using a wound healing assay (25). Briefly, $3x10^5$ cells/well were seeded into 6-well plates and cultured until they reached 90% confluence. After which, a sterile pipette tip was used to scratch across the center of each well, creating a defined wound area. Detached cells were removed by washing with 500 μl PBS and fresh culture medium was added. Subsequently, cell migration into the scratched area was monitored and captured at 0 and 24 h using a Nikon E 600 phase-contrast microscope. Images of the wound area were analyzed using ImageJ software (version 2.9.0/1.53t; National Institutes of Health) (26). Wound closure percentage was calculated as $[(A_{t=0}-At_{=\Delta t})/A_{t=0}]$ x100, where $A_{t=0}$ is the scratch area at 0 h and $At_{=\Delta t}$ is the scratch area at 24 h.

RNA extraction and reverse transcription-quantitative PCR (RT-qPCR). RNA was isolated in accordance with the manufacturer's protocol using an RNA extraction kit (cat. no. R1200; Beijing Solarbio Science & Technology Co., Ltd.). Subsequently, cDNA was synthesized using random nonamer primers and the First-Strand Synthesis System (MilliporeSigma; Merck KGaA). EvaGreen fluorescence-based RT-qPCR was performed using reagents purchased from Applied Biological Materials, Inc. RT-qPCR reactions were performed following standard protocols as previously described (27). The RT-qPCR primers used in the present study are listed in Table I. The gene expression

Table I. Primers for RT-qPCR used in the present study.

Gene symbol	Oligo sequence (5'-3')
AF-6 (AFDN)	F: AGTCGGTTGTGAAAGGAGGTGC
	R: TCCTGAGAGAGTCCAACCAGAC
APC	F: AGGCTGCATGAGAGCACTTGTG
	R: CACACTTCCAACTTCTCGCAACG
Bax	F: TCAGGATGCGTCCACCAAGAAG
	R: TGTGTCCACGGCGGCAATCATC
Bcl-2	F: ATCGCCCTGTGGATGACTGAGT
	R: GCCAGGAGAAATCAAACAGAGGC
Bcl-6	F: CATGCAGAGATGTGCCTCCACA
	R: TCAGAGAAGCGGCAGTCACACT
Caspase 3	F: GGAAGCGAATCAATGGACTCTGG
	R: GCATCGACATCTGTACCAGACC
CDK4	F: CCATCAGCACAGTTCGTGAGGT
	R: TCAGTTCGGGATGTGGCACAGA
CLDN2	F: GTGACAGCAGTTGGCTTCTCCA
	R: GGAGATTGCACTGGATGTCACC
CLDN14	F: CCAAGACCACCTTTGCCATCCT
	R: AGTTCTGCACCACGTCGTTGGT
CLDN23	F: CCTGGTGCGACGAGCGTTGTC
	R: GTCGCTGTAGTACTTGATGGCG
IL-6	F: AGACAGCCACTCACCTCTTCAG
	R: TTCTGCCAGTGCCTCTTTGCTG
MMP7	F: TCGGAGGAGATGCTCACTTCGA
	R: GGATCAGAGGAATGTCCCATACC
NDRG1	F: ATCACCCAGCACTTTGCCGTCT
	R: GACTCCAGGAAGCATTTCAGCC
p53	F: CCTCAGCATCTTATCCGAGTGG
	R: TGGATGGTGGTACAGTCAGAGC
PTMS	F: AGAAACTGCCGAGGATGGAGAG
	R: TGCCGTTTGGGATCCGCTTCAT
TCN1	F: CAGTGTGATGGAGAAAGCCCAG
	R: CCACTCAGAAGTTCCCAGTAGG
VDR	F: CGCATCATTGCCATACTGCTGG
	R: CCACCATCATTCACACGAACTGG
ZO-1 (TJP1)	F: GTCCAGAATCTCGGAAAAGTGCC
	R: CTTTCAGCGCACCATACCAACC
ZONAB (YBX3)	F: TGGTCCAAACCAGCCGTCTGTT
	R: GTTCTCAGTTGGTGCTTCACCTG
GAPDH (RG)	F: GTCTCCTCTGACTTCAACAGCG
	R: ACCACCCTGTTGCTGTAGCCAA

RG, reference gene; RT-qPCR, reverse transcription-quantitative PCR; F, forward; R, reverse; CLDN2, claudin-2; *ZO-1*, zonula occludens-1; *VDR*, vitamin D receptor; *ZONAB*, ZO-1-associated nucleic acid binding protein; *YBX3*, Y-box binding protein 3; *NDRG1*, N-Myc downstream-regulated gene 1; *APC*, adenomatous polyposis coli; *AF-6*/*AFDN*, Afadin; TJP1, tight junction protein 1; *PTMS*, parathymosin; TCN-1, transcobalamin 1.

levels in the samples were investigated using RT-qPCR and the cDNA synthesis and PCR procedures were optimized to ensure high-quality results.

Relative and normalized fold expression values calculation. The gene expression patterns of several target genes were examined in samples from both Wt and *CLDN2*-KO cells using RT-qPCR. Relative expression levels were calculated using the comparative Cq method (ΔΔCq), normalized to GAPDH as the reference gene (28). For every target gene, the Cq values that were derived from the amplification curves were used to compute ΔCq, copy number, ΔΔCq and fold change. ΔCq was calculated using the following formula: $\Delta Cq=Cq_{(\text{target gene; same sample})}-Cq_{(\text{control gene; same sample})}$. Copy number was calculated using the following formula: Copy number=100 x $2^{-\Delta Cq}$. ΔΔCq was calculated using the following formula: $\Delta\Delta Cq=\Delta Cq_{(\text{same gene; target sample})}-\Delta Cq_{(\text{same gene; control sample})}$. Fold change was calculated using the following formula: Fold change=$2^{-\Delta\Delta Cq}$.

The housekeeping gene *GAPDH* was used as an internal control for normalization. The expression levels of *GAPDH* were relatively stable across all samples. Data are represented as the mean of three independent experiments.

Statistical analysis. Statistical analyses were performed using GraphPad Prism software (version 8.0; Dotmatics). Data are presented as the mean ± SEM, with at least three independent biological replicates. Normality was assessed using the Shapiro-Wilk test. Statistical significance was assessed using Welch's unpaired t-test for ΔCq values Comparisons between two groups (Wt vs. *CLDN2*-KO) were made using an unpaired two-tailed Student's t-test if data were normally distributed or a Mann-Whitney U test for non-parametric comparisons. $P<0.05$ was considered to indicate a statistically significant difference.

Results

High efficiency of CRISPR/Cas9 editing of the CLDN2 gene. The Synthego ICE CRISPR Analysis tool was employed to assess the effectiveness of CRISPR *CLDN2* gene KO (Fig. 1). The ICE value of 91% indicated a high degree of editing efficiency, suggesting that a notable proportion of the cells within the edited population harbored the intended *CLDN2* gene KO. Particularly, 91% of cells contained the indel of the *CLDN2* gene after CRISPR/Cas9 editing.

Fig. 2 presents the Sanger sequencing discordance plot, comparing sequencing traces from Wt and *CLDN2*-KO cells around the CRISPR cut site. Prior to the cut site, the Wt and *CLDN2*-KO traces overlapped. At the target site, a sharp increase in sequence discordance was observed in *CLDN2*-KO cells, evidenced by the divergence between Wt (green) and *CLDN2*-KO (orange) signal lines. This pattern is characteristic of successful genome editing. Furthermore, Fig. 3 displays the Sanger sequence alignment surrounding the sgRNA target site, with the sgRNA sequence underlined in black and the protospacer adjacent motif underlined in red. A vertical line marks the cut site, where sequence differences between Wt and *CLDN2*-KO cells become evident. These results confirmed that the *CLDN2* gene was effectively knocked out in HCT116 cells with high efficiency. Consistent with the sequencing results, qPCR analysis demonstrated a significant reduction in *CLDN2* expression in *CLDN2*-KO cells relative to Wt cells (Fig. S1).

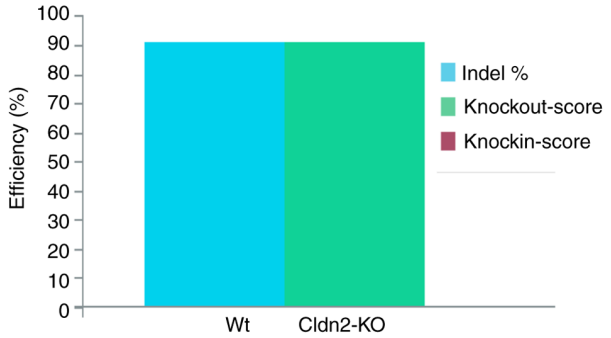

Figure 1. ICE analysis of CRISPR/Cas9-mediated *CLDN2*-KO efficiency in HCT116 cells. ICE software analysis confirmed successful editing of the *CLDN2* locus with an efficiency of ~91%. The editing score reflects the proportion of indels detected in the cell population. ICE, Inference of CRISPR Edits; *CLDN2*, claudin-2; Wt, wild-type; KO, knockout; indel, insertion-deletion.

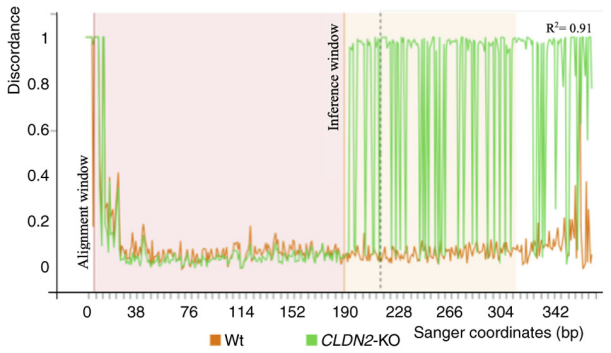

Figure 2. Sanger discordance plot displays the alignment/base between the Wt and *CLDN2*-KO samples and inside the inference window (the area around the cute site) indicates the average proportion of signal that differs from the reference sequence obtained from the Wt trace. In the plot, the proximity between the green line and orange line is seen before to the cut site. However, a typical CRISPR edit leads to a notable increase in sequence discordance at the cut site, causing the green and orange lines to stay far apart afterwards. Wt, wild-type; *CLDN2*-KO, claudin-2 knockout.

CLDN2-KO impairs HCT116 cell migration. At 24 h, Wt cells exhibited near-complete wound closure (~96%), while *CLDN2*-KO cells achieved only ~41% closure. Quantification of wound healing (Fig. 4B) demonstrated a significant reduction in migratory capacity in *CLDN2*-KO cells compared with Wt controls (P=0.0027; unpaired t-test; n=3 independent experiments). These findings indicated that *CLDN2* is key for the efficient migration of CRC cells.

Gene expression profiles in Wt and CLDN2-KO samples. To investigate the transcriptional effects of *CLDN2* deletion, the expression levels of multiple genes implicated in invasion and metastasis was analyzed using RT-qPCR. Fig. 5 displays the copy numbers of target genes in Wt and *CLDN2*-KO cells. Analysis of copy number variations for all genes consistently demonstrated a significant decrease in copy number in *CLDN2*-KO samples compared with the Wt cells (all P<0.05). The observed patterns indicated that *CLDN2*-KO has a notable impact on its interacting partners, causing their downregulation.

Fig. 6 depicts the fold-change values of several genes in both Wt and *CLDN2*-KO samples. Of all the genes that were evaluated, *IL-6* was the least downregulated in *CLDN2*-KO samples, with a fold-change of 0.718 and maintains a relatively stable expression pattern. By contrast, *AF-6*, which encodes Afadin, exhibited the most marked downregulation, with a fold-change of 0.008. These results suggested that *CLDN2* loss disrupts a network of pro-metastatic gene expression programs that may contribute to impaired cellular migration and reduced metastatic potential.

Discussion

Claudins are key components of tight junctions, serving key roles in the maintenance of epithelial integrity and regulating paracellular permeability (8). Previous studies have suggested that claudins are involved in the development of malignancies. However, the specific process has not yet been fully elucidated (9,29,30).

In the present study, the role of *CLDN2* in CRC progression was investigated. Using CRISPR/Cas9-mediated *CLDN2*-KO in HCT116 cells, it was demonstrated that the loss of *CLDN2* leads to significant downregulation of genes associated with invasion, metastasis and cell motility. The findings of the present study aligned with previous studies suggesting that *CLDN2* promotes tumorigenicity and metastasis in CRC (8-11,26,31). Particularly, it was observed that *CLDN2*-KO resulted in significantly reduced expression levels of ZONAB and NDRG1, two factors which regulate epithelial proliferation and metastasis suppression, respectively.

ZONAB is a Y-box transcription factor that interacts with the tight junction protein *ZO-1*. When retained at tight junctions, its transcriptional activity is restricted, whereas nuclear translocation of ZONAB promotes the expression levels of genes involved in proliferation and epithelial-mesenchymal transition (32,33). By contrast, NDRG1 functions as a metastasis suppressor. It inhibits invasion and migration, modulates epithelial differentiation and negatively regulates oncogenic pathways such as *PI3K/AKT* and Wnt/β-catenin (34,35). Downregulation of *NDRG1* is associated with poor prognosis in CRC (13). Thus, *CLDN2*-driven suppression of *NDRG1* through ZONAB activity provides a mechanistic association between tight junction dysregulation and enhanced tumor progression. These results support the hypothesis that *CLDN2* may modulate the CLDN2/*ZO-1*/ZONAB signaling axis, thereby influencing transcriptional programs key for cancer cell migration and invasion (36). Previous studies suggested that the abundance of *CLDN2* increases with cell confluence and the maturation of tight junctions and that *ZO-1* (and *ZO-2)* help stabilize *CLDN2* by reducing its turnover. Knockdown of *ZO-1* leads to notable loss of *CLDN2* abundance and promoter activity (37). In the present study, the downregulation of *ZO-1* in *CLDN2*-KO cells indicated that downstream signaling is disrupted in the absence of *CLDN2*.

In addition to tight junction-related proteins, *CLDN2*-KO affected the expression levels of other metastasis-associated genes. Downregulation of *CLDN14* and *CLDN23*, tight junction components previously associated with CRC progression (38,39), was observed. Furthermore, reduced expression level of *AF-6* (encoding Afadin), a scaffolding protein involved

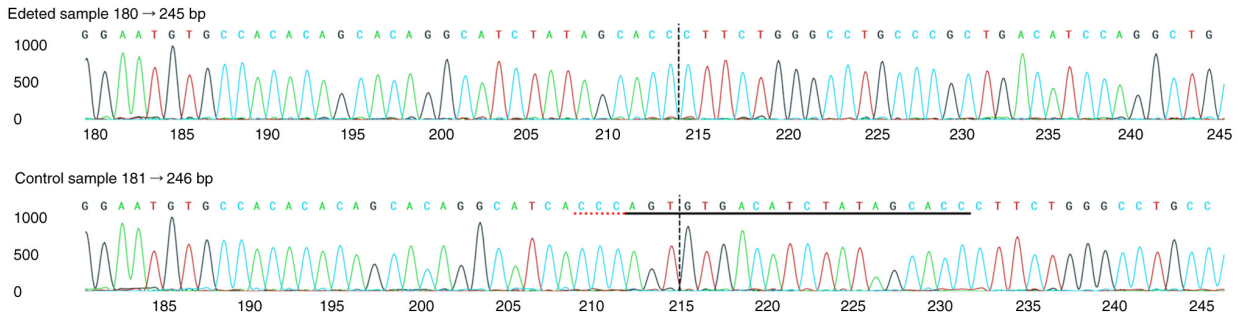

Figure 3. Sanger sequence view displays the knockout and Wt sequences in the immediate area of the guide sequence. This displays the sequence base calls obtained from Wt) and *CLDN2*-KO). The guide sequence is represented by the horizontal black underlined section. The PAM location is indicated with a horizontal red underline. The vertical line, indicated by the black dots, depicts the precise location of the incision. Performing a cut and attempting to repair it often leads to the presence of mixed sequencing bases. PAM, protospacer adjacent motif; Wt, wild-type; *CLDN2*-KO, claudin-2 knockout.

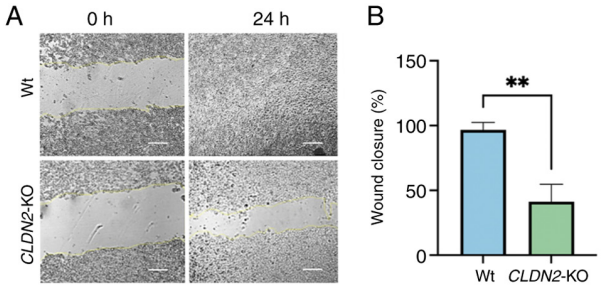

Figure 4. Wound healing assay assessing cell migration in Wt and *CLDN2*-KO HCT116 cells. (A) Representative images of wound closure at 0 and 24 h post-scratch (scale bar, 100 μm). (B) Quantification of wound closure percentage. Wt cells achieved ~96% closure, while *CLDN2*-KO cells demonstrated 41% closure after 24 h (P=0.0027; unpaired two-tailed t-test; n=3). Data are presented as the mean ± SEM. **P<0.01. Wt, wild-type; *CLDN2*-KO, claudin-2 knock out.

in cell-cell adhesion and migration, was also notable. Previous research has demonstrated that *CLDN2* physically interacts with Afadin via its PDZ-binding motif and this complex contributes to metastatic behavior in breast cancer models. In addition, loss of Afadin impairs colony formation and metastasis (40,41). This provides a precedent to consider a *CLDN2*-Afadin axis in CRC.

Furthermore, the data in the present study revealed a decreased expression level of CDK4, a cyclin-dependent kinase key for cell cycle progression. Since ZONAB (regulated by *CLDN2*) can associate with and influence CDK4 nuclear activity, reduced *CDK4* expression may reflect the disruption of *CLDN2*/*ZO-1*/ZONAB signaling (32,33,42). Collectively, these transcriptional changes highlight the broad regulatory influence of *CLDN2* on multiple pathways driving CRC metastasis.

Notably, several key oncogenic and tumor suppressor genes were also modulated by *CLDN2* deletion. The proto-oncogene c-*Myc*, a master regulator of proliferation and metabolism, was significantly downregulated. Reduced c-*Myc* expression may contribute to the suppression of migratory and invasive phenotypes in *CLDN2*-deficient cells, consistent with its role in CRC aggressiveness (43).

An inverse association between *p53* and *CLDN2* has been reported in mouse colon tissue during dextran sulfate sodium-induced colitis (44), where reduced *p53* expression was accompanied by increased *CLDN2* levels, suggesting that loss of *p53*-mediated regulation may contribute to *CLDN2* upregulation in inflamed and neoplastic intestinal epithelium (45). Furthermore, a previous study suggested a negative regulatory complex involving *p53* and hepatocyte nuclear factor 4 α that may influence *CLDN2* expression (44). However, in the present study, downregulation of *p53* in the KO condition, indicated by a fold-change of 0.02, suggests that *CLDN2* may have a regulatory role in its own expression. The reduced copy number further supports the notion of downregulation of *p53* in the *CLDN2*-KO cells.

A previous study provided evidence for the qualitative and quantitative expression levels of *Bcl-6* involvement in human CRC progression, and demonstrated that *Bcl-6* appears to be involved in tumor development, from the earliest stage of carcinogenesis (46). In the present study, in the KO condition, *Bcl-6* exhibited a downregulation, indicating a possible regulatory function for *CLDN2* in its expression. Although direct evidence of a *CLDN2*-*Bcl-6* axis is limited, to the best of our knowledge, perturbations in tight junction integrity and nuclear signaling have been associated with transcriptional repressor modulation in cancer (47,48), suggesting that *CLDN2* loss may indirectly influence *Bcl-6* expression.

Furthermore, the tumor suppressor gene adenomatous polyposis coli (APC), a key component of the Wnt/β-catenin signaling pathway, was markedly reduced. APC dysfunction is a hallmark of CRC initiation and progression (49,50). Its downregulation following *CLDN2*-KO highlights the complex interplay between tight junction integrity and oncogenic pathways. Loss of APC may also reflect feedback from junctional disruption on Wnt signaling regulation, further implicating *CLDN2* in the modulation of oncogenic cascades. Activation of the Wnt/β-catenin signaling pathway has been documented in a notable proportion of gastric cancer cases. For example, nuclear β-catenin accumulation, a hallmark of Wnt pathway activation, has been reported in ~1/3 of gastric adenocarcinomas (51). Recent studies estimated that 30-50% of gastric tumor specimens exhibit hyperactivation of this pathway (52,53). In addition, activation of Wnt/β-catenin signaling has been reported to increase the expression levels of *MMP7* at both the mRNA and protein levels in triple-negative breast cancer, providing a mechanistic association between Wnt signaling and invasive phenotypes (54,55). These findings further support the role

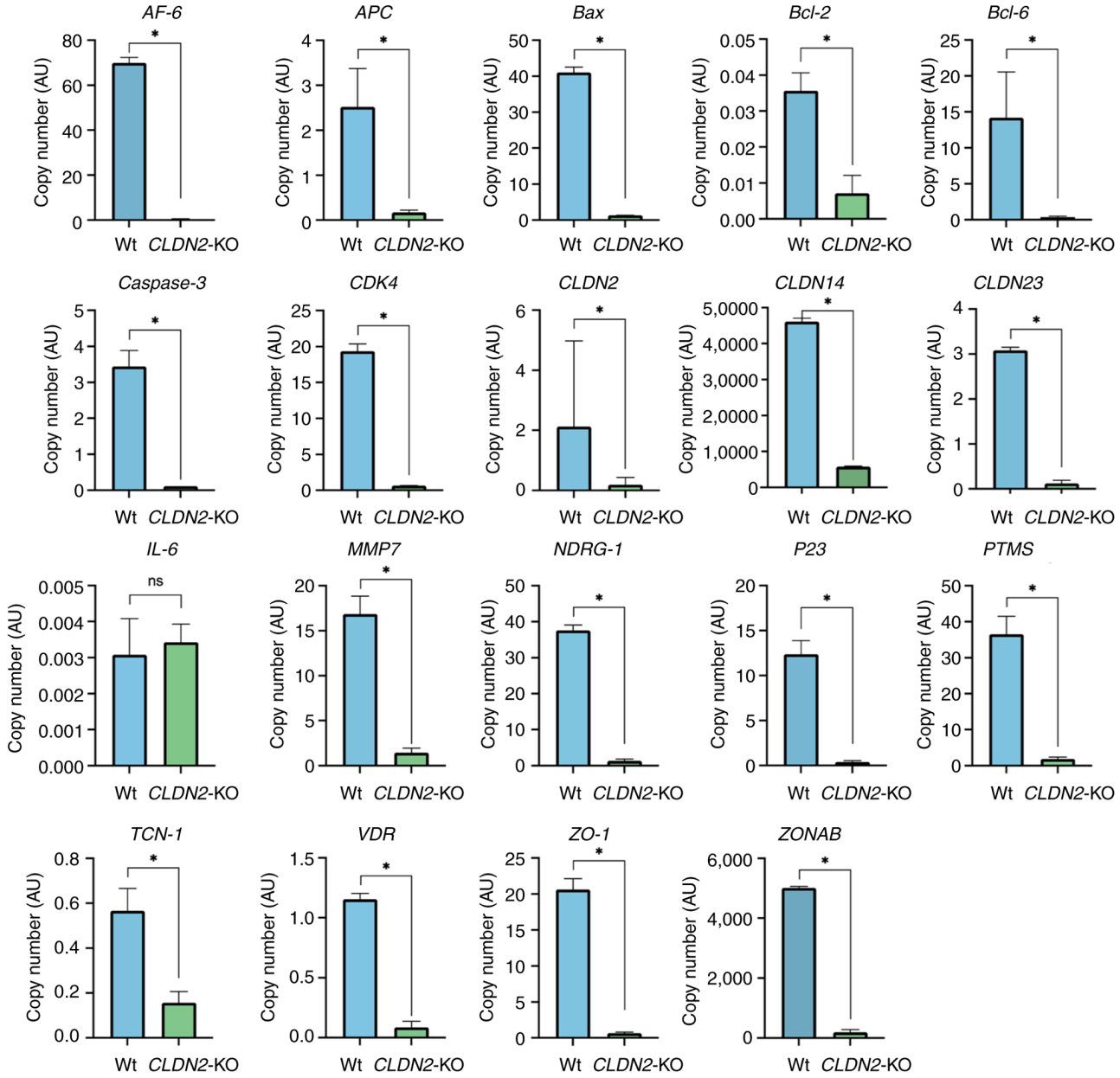

Figure 5. Gene expression analysis of invasion- and metastasis-related genes in *CLDN2*-KO vs. Wt HCT116 cells. Reverse transcription-quantitative PCR exhibited significant downregulation of multiple target genes, including *ZONAB, NDRG1*, *CLDN14*, *CLDN23*, *Bcl-2, p53* and *Bcl-6*. Gene expression levels were normalized to GAPDH. Data are represented as mean ± SEM (n=3). Statistical comparisons were made using unpaired two-tailed t-tests. *P<0.05. ns, not significant; Wt, wild-type; *CLDN2*-KO, claudin-2 knock out; ZO-1, zonula occludens-1; *VDR*, vitamin D receptor; *ZONAB, ZO-1*-associated nucleic acid binding protein; NDRG1, N-Myc downstream-regulated gene 1; APC, adenomatous polyposis coli; *AF-6/AFDN*, Afadin; TJP1, tight junction protein 1; YBX3, Y-box binding protein 3; PTMS, parathymosin; TCN-1, transcobalamin 1.

of Wnt pathway activation in promoting cancer progression across multiple tumor types.

Furthermore, the vitamin D receptor (VDR), which regulates proliferation, differentiation and epithelial barrier function, exhibited decreased expression. Multiple studies have indicated that *VDR* can directly bind and regulate *CLDN2* transcription in intestinal tissues, and that *VDR* dysregulation has been implicated in colorectal tumorigenesis (56,57). This supports a bidirectional regulatory association between *VDR* and *CLDN2* expression, and suggests that *CLDN2* loss may contribute to impaired *VDR* signaling in CRC.

Notably, elevated *CLDN2* expression has been associated with poor prognosis in CRC, liver cancer and other gastrointestinal malignancies (7,12,58). The findings of the present study supported this clinical association by demonstrating that Cldn2 loss impairs migratory potential and suppresses pro-metastatic gene expression. Thus, targeting *CLDN2* may represent a promising therapeutic strategy to inhibit CRC metastasis in the future, although careful evaluation of potential side effects on normal epithelial function is warranted in future studies.

It is key to acknowledge the limitations of the present study. While the present study results demonstrated a strong association between *CLDN2* loss and altered gene expression, mechanistic experiments, such as rescue assays or pathway-specific inhibition, were not performed to directly

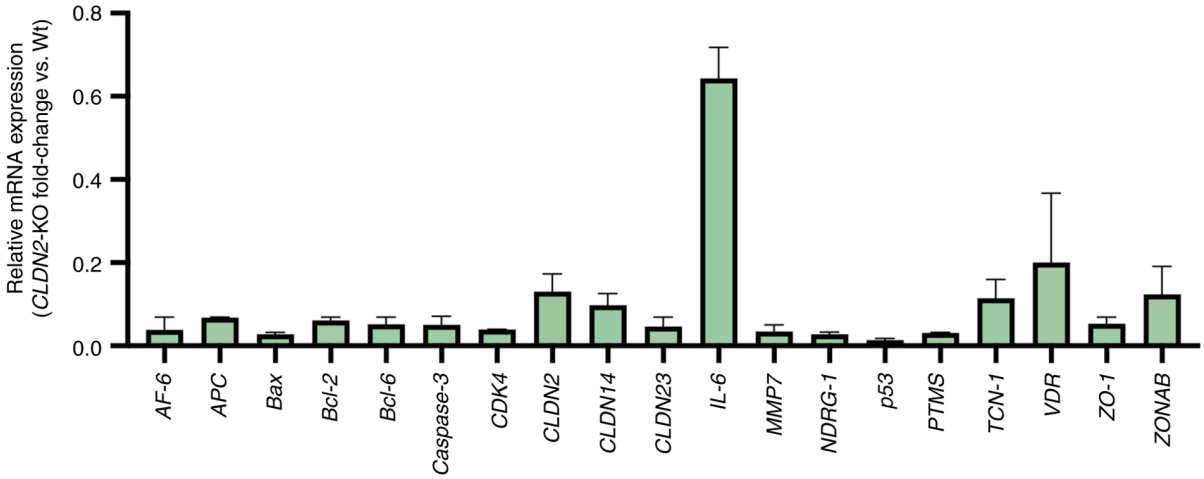

Figure 6. Relative expression levels of metastasis-associated genes in Wt and *CLDN2*-KO HCT116 cells. Gene expression was quantified using reverse transcription-quantitative PCR. Each bar represents the mean ± SEM of three independent experiments. Values were calculated using the $2^{-\Delta\Delta Cq}$ method and normalized to GAPDH. Expression in Wt cells was set to 1.0 and knock out values were expressed relative to this baseline. Each bar corresponds to a specific gene and the height of the bars indicates the magnitude of the fold-change observed in the *CLDN2*-KO samples compared with the Wt samples. The highest bars on the figure represent the gene with the lowest degree of expression variation. *IL-6* exhibited the lowest degree of downregulation (fold-change, 0.718), whereas AF-6 demonstrated the most pronounced reduction (fold-change, 0.008). Wt, wild type; *ZO-1*, zonula occludens-1; *VDR*, vitamin D receptor; *ZONAB*, ZO-1-associated nucleic acid binding protein; NDRG1, N-Myc downstream-regulated gene 1; APC, adenomatous polyposis coli; *AF-6*, Afadin; PTMS, parathymosin; TCN-1, transcobalamin 1; *CLDN2*-KO, claudin-2 knock out; AU, arbitrary Units.

establish causality. The findings were also based on *in vitro* analyses in a single CRC cell line; validation using *in vivo* models or additional cell lines in future studies would strengthen these conclusions. Another limitation is that *CLDN2* protein loss was not validated by western blotting, although the CRISPR editing efficiency was demonstrated by qPCR, ICE analysis and Sanger sequencing. In addition, cell migration was assessed only by the wound healing assay. While this method reflects overall migratory capacity, it does not capture chemotactic or invasive behavior. Incorporating approaches such as Transwell migration and invasion assays would provide complementary evidence and these are planned for future research. Lastly, further studies are warranted to dissect the downstream mechanisms by which *CLDN2* modulates signaling pathways. Rescue experiments restoring *CLDN2* expression, pathway-specific analyses (such as PI3K/AKT, Wnt/β-catenin and yes-associated protein/transcriptional co-activator with PDZ-binding motif) and investigation of the interaction partners of *CLDN2*, such as ZONAB and Afadin, will be key to elucidate its precise role in CRC progression in the future.

In conclusion, the present study demonstrated that *CLDN2* serves a key role in regulating metastasis-associated gene networks in CRC. Disruption of *CLDN2* in HCT116 cells significantly impaired migration and was accompanied by the downregulation of key invasion- and metastasis-related genes, including *ZONAB, NDRG1, AF-6*, *CLDN14*, *CLDN23*, *CDK4*, Bcl-*6* and *APC*. These transcriptional changes highlight the broad regulatory influence of *CLDN2* on pathways governing cell adhesion, proliferation and Wnt/β-catenin signaling. While additional mechanistic studies, such as rescue assays and pathway-specific analyses, are warranted to further dissect these interactions, the present study findings provide notable genetic and phenotypic evidence that *CLDN2* contributes to CRC progression. By directly associating *CLDN2* deletion with the suppression of specific pro-metastatic genes, the present study suggests that targeting *CLDN2* may represent a promising therapeutic strategy to potentially inhibit CRC metastasis in the future.

Acknowledgements

Not applicable.

Funding

The present study was funded by the Deanship of Scientific Research (DSR) at King Abdulaziz University, Jeddah, Saudi Arabia (grant no. G: 48-665-1443).

Availability of data and materials

The data generated in the present study may be requested from the corresponding author.

Authors' contributions

RA conceived and designed the study. MA designed the study. RA and MA performed experiments, analyzed and interpreted the data and wrote the manuscript. RA and MA confirm the authenticity of all the raw data. Both authors have read and approved the final manuscript.

Ethics approval and consent to participate

Not applicable.

Patient consent for publication

Not applicable.

Competing interests

The authors declare that they have no competing interests.

Use of artificial intelligence tools

During the preparation of this work, artificial intelligence tools were used to improve the readability and language of the manuscript or to generate images, and subsequently, the authors revised and edited the content produced by the artificial intelligence tools as necessary, taking full responsibility for the ultimate content of the present manuscript.

References

1. Siegel RL, Wagle NS, Cercek A, Smith RA and Jemal A: Colorectal cancer statistics, 2023. CA Cancer J Clin 73: 233-254, 2023.
2. Xi Y and Xu P: Global colorectal cancer burden in 2020 and projections to 2040. Transl Oncol 14: 101174, 2021.
3. Mousavi SE, Ilaghi M, Hamidi Rad R and Nejadghaderi SA: Epidemiology and socioeconomic correlates of colorectal cancer in Asia in 2020 and its projection to 2040. Sci Rep 15: 26639, 2025.
4. Sarkar S: Proteogenomic approaches to understand gene mutations and protein structural alterations in colon cancer. Physiologia 3: 11-29, 2023.
5. Tabariès S, Dupuy F, Dong Z, Monast A, Annis MG, Spicer J, Ferri LE, Omeroglu A, Basik M, Amir E, *et al*: Claudin-2 promotes breast cancer liver metastasis by facilitating tumor cell interactions with hepatocytes. Mol Cell Biol 32: 2979-2991, 2012.
6. Cherradi S, Ayrolles-Torro A, Vezzo-Vié N, Gueguinou N, Denis V, Combes E, Boissière F, Busson M, Canterel-Thouennon L, Mollevi C, *et al*: Antibody targeting of claudin-1 as a potential colorectal cancer therapy. J Exp Clin Cancer Res 36: 89, 2017.
7. Tabariès S, Annis MG, Lazaris A, Petrillo SK, Huxham J, Abdellatif A, Palmieri V, Chabot J, Johnson RM, Van Laere S, *et al*: Claudin-2 promotes colorectal cancer liver metastasis and is a biomarker of the replacement type growth pattern. Commun Biol 4: 657, 2021.
8. Venugopal S, Anwer S and Szászi K: Claudin-2: Roles beyond permeability functions. Int J Mol Sci 20: 5655, 2019.
9. Alghamdi RA and Al-Zahrani MH: Identification of key claudin genes associated with survival prognosis and diagnosis in colon cancer through integrated bioinformatic analysis. Front Genet 14: 1221815, 2023.
10. Weber CR, Nalle SC, Tretiakova M, Rubin DT and Turner JR: Claudin-1 and claudin-2 expression is elevated in inflammatory bowel disease and may contribute to early neoplastic transformation. Lab Invest 88: 1110-120, 2008.
11. Rosenthal R, Milatz S, Krug SM, Oelrich B, Schulzke JD, Amasheh S, Günzel D and Fromm M: Claudin-2, a component of the tight junction, forms a paracellular water channel. J Cell Sci 123: 1913-1921, 2010.
12. Dhawan P, Ahmad R, Chaturvedi R, Smith JJ, Midha R, Mittal MK, Krishnan M, Chen X, Eschrich S, Yeatman TJ, *et al*: Claudin-2 expression increases tumorigenicity of colon cancer cells: Role of epidermal growth factor receptor activation. Oncogene 30: 3234-3247, 2011.
13. Wei M, Zhang Y, Yang X, Ma P, Li Y, Wu Y, Chen X, Deng X, Yang T, Mao X, *et al*: Claudin-2 promotes colorectal cancer growth and metastasis by suppressing NDRG1 transcription. Clin Transl Med 11: e667, 2021.
14. Al-Zahrani M, Lary S, Assidi M, Hakamy S, Dallol A, Alahwal M, Al-Maghrabi J, Sibiany A, Abuzenadah A, Al-Qahtani M and Buhmeida A: Evaluation of prognostic potential of CD44, Claudin-2 and EpCAM expression patterns in colorectal carcinoma. Adv Environmental Biol 10: 147-156, 2016.
15. Vogelstein B, Papadopoulos N, Velculescu VE, Zhou S, Diaz LA Jr and Kinzler KW: Cancer genome landscapes. Science 339: 1546-1558, 2013.
16. Kim D and Cho KH: Hidden patterns of gene expression provide prognostic insight for colorectal cancer. Cancer Gene Ther 30: 11-21, 2022.
17. Cancer Genome Atlas Network: Comprehensive molecular characterization of human colon and rectal cancer. Nature 487: 330-337, 2012.
18. Zhao Z, Li C, Tong F, Deng J, Huang G and Sang Y: Review of applications of CRISPR-Cas9 gene-editing technology in cancer research. Biol Proced Online 23: 14, 2021.
19. Meng H, Nan M, Li Y, Ding Y, Yin Y and Zhang M: Application of CRISPR-Cas9 gene editing technology in basic research, diagnosis and treatment of colon cancer. Front Endocrinol (Lausanne) 14: 1148412, 2023.
20. Neumann E, Schaefer-Ridder M, Wang Y and Hofschneider P: Gene transfer into mouse lyoma cells by electroporation in high electric fields. EMBO J 1: 841-845, 1982.
21. Enzmann BL and Wronski A: Synthego's engineered cells allow scientists to 'Cut Out' CRISPR optimization [SPONSORED]. CRISPR J 1: 255-257, 2018.
22. Roginsky J: Analyzing CRISPR editing results: Synthego developed a tool called ICE to be more efficient than other methods. Genet Eng Biotechnol News 38 (Suppl): S24-S26, 2018.
23. Bentley DR, Balasubramanian S, Swerdlow HP, Smith GP, Milton J, Brown CG, Hall KP, Evers DJ, Barnes CL, Bignell HR, *et al*: Accurate whole human genome sequencing using reversible terminator chemistry. Nature 456: 53-59, 2008.
24. Gross A, Schoendube J, Zimmermann S, Steeb M, Zengerle R and Koltay P: Technologies for single-cell isolation. Int J Mol Sci 16: 16897-16919, 2015.
25. Liang CC, Park AY and Guan JL: In vitro scratch assay: A convenient and inexpensive method for analysis of cell migration in vitro. Nat Protoc 2: 329-333, 2007.
26. Schneider CA, Rasband WS and Eliceiri KW: NIH Image to ImageJ: 25 years of image analysis. Nat Methods 9: 671-675, 2012.
27. Bustin SA, Benes V, Garson JA, Hellemans J, Huggett J, Kubista M, Mueller R, Nolan T, Pfaffl MW, Shipley GL, *et al*: The MIQE guidelines: Minimum information for publication of quantitative real-time PCR experiments. Clin Chem 55: 611-622, 2009.
28. Livak KJ and Schmittgen TD: Analysis of relative gene expression data using real-time quantitative PCR and the 2(-Delta Delta C(T)) Method 25: 402-408, 2001.
29. Zhu L, Han J, Li L, Wang Y, Li Y and Zhang S: Claudin family participates in the pathogenesis of inflammatory bowel diseases and Colitis-associated colorectal cancer. Front Immunol 10: 1441, 2019.
30. Al-Zahrani MH, Assidi M, Pushparaj PN, Al-Maghrabi J, Zari A, Abusanad A, Buhmeida A and Abu-Elmagd M: Expression pattern, prognostic value and potential microRNA silencing of FZD8 in breast cancer. Oncol Lett 26: 477, 2023.
31. Ahmad R, Kumar B, Thapa I, Tamang RL, Yadav SK, Washington MK, Talmon GA, Yu AS, Bastola DK, Dhawan P and Singh AB: Claudin-2 protects against colitis-associated cancer by promoting colitis-associated mucosal healing. J Clin Invest 133: e170771, 2023.
32. Sourisseau T, Georgiadis A, Tsapara A, Ali RR, Pestell R, Matter K and Balda MS: Regulation of PCNA and Cyclin D1 expression and epithelial morphogenesis by the ZO-1-regulated transcription factor ZONAB/DbpA. Mol Cell Biol 26: 2387-2398, 2006.
33. Balda MS: The tight junction protein ZO-1 and an interacting transcription factor regulate ErbB-2 expression. EMBO J 19: 2024-2033, 2000.
34. Kovacevic Z and Richardson DR: The metastasis suppressor, Ndrg-1: A new ally in the fight against cancer. Carcinogenesis 27: 2355-2366, 2006.
35. Sun J, Zhang D, Bae DH, Sahni S, Jansson P, Zheng Y, Zhao Q, Yue F, Zheng M, Kovacevic Z and Richardson DR: Metastasis suppressor, NDRG1, mediates its activity through signaling pathways and molecular motors. Carcinogenesis 34: 1943-1954, 2013.
36. Tao D, Guan B, Li H and Zhou C: Expression patterns of claudins in cancer. Heliyon 9: e21338, 2023.
37. Amoozadeh Y, Anwer S, Dan Q, Venugopal S, Shi Y, Branchard E, Liedtke E, Ailenberg M, Rotstein OD, Kapus A and Szászi K: Cell confluence regulates claudin-2 expression: Possible role for ZO-1 and Rac. Am J Physiol Physiol 314: C366-C378, 2018.
38. Yang L, Zhang W, Li M, Dam J, Huang K, Wang Y, Qiu Z, Sun T, Chen P, Zhang Z and Zhang W: Evaluation of the prognostic relevance of differential claudin gene expression highlights Claudin-4 as Being Suppressed by TGFβ1 inhibitor in colorectal cancer. Front Genet 13: 783016, 2022.

39. Chen W, Zhu XN, Wang J, Wang YP and Yang JL: The expression and biological function of claudin-23 in colorectal cancer. Sichuan Da Xue Xue Bao Yi Xue Ban 49: 331-336, 2018 (In Chinese).
40. Tabariès S, McNulty A, Ouellet V, Annis MG, Dessureault M, Vinette M, Hachem Y, Lavoie B, Omeroglu A, Simon HG, *et al*: Afadin cooperates with Claudin-2 to promote breast cancer metastasis. Genes Dev 33: 180-193, 2019.
41. Zhang X, Wang H, Li Q and Li T: CLDN2 inhibits the metastasis of osteosarcoma cells via down-regulating the afadin/ERK signaling pathway. Cancer Cell Int 18: 160, 2018
42. González-Mariscal L, Miranda J, Gallego-Gutiérrez H, Cano-Cortina M and Amaya E: Relationship between apical junction proteins, gene expression and cancer. Biochim Biophys Acta Biomembr 1862: 183278, 2020.
43. Dang CV: MYC on the path to cancer. Cell 149: 22-35, 2012.
44. Hirota C, Takashina Y, Ikumi N, Ishizuka N, Hayashi H, Tabuchi Y, Yoshino Y, Matsunaga T and Ikari A: Inverse regulation of claudin-2 and -7 expression by p53 and hepatocyte nuclear factor 4α in colonic MCE301 cells. Tissue Barriers 9: 1860409, 2021.
45. Kim HY, Jeon H, Bae CH, Lee Y, Kim H and Kim S: Rumex japonicus Houtt. alleviates dextran sulfate sodium-induced colitis by protecting tight junctions in mice. Integr Med Res 9: 100398, 2020.
46. Sena P, Mariani F, Benincasa M, De Leon MP, Di Gregorio C, Mancini S, Cavani F, Smargiassi A, Palumbo C and Roncucci L: Morphological and quantitative analysis of BCL6 expression in human colorectal carcinogenesis. Oncol Rep 31: 103-110, 2014.
47. Li J: Context-dependent roles of claudins in tumorigenesis. Front Oncol 11: 676781, 2021.
48. Nehme Z, Roehlen N, Dhawan P and Baumert TF: Tight junction protein signaling and cancer biology. Cells 12: 243, 2023.
49. Miwa N, Furuse M, Tsukita S, Niikawa N, Nakamura Y and Furukawa Y: Involvement of claudin-1 in the beta-catenin/Tcf signaling pathway and its frequent upregulation in human colorectal cancers. Oncol Res 12: 469-476, 2001.
50. Mankertz J, Hillenbrand B, Tavalali S, Huber O, Fromm M and Schulzke JD: Functional crosstalk between Wnt signaling and Cdx-related transcriptional activation in the regulation of the claudin-2 promoter activity. Biochem Biophys Res Commun 314: 1001-1007, 2004.
51. Clements WM, Wang J, Sarnaik A, Kim OJ, MacDonald J, Fenoglio-Preiser C, Groden J and Lowy AM: Beta-Catenin mutation is a frequent cause of Wnt pathway activation in gastric cancer. Cancer Res 62: 3503-3506, 2002.
52. Chiurillo MA: Role of the Wnt/β-catenin pathway in gastric cancer: An in-depth literature review. World J Exp Med 5: 84-102, 2015.
53. Jang JH, Jung J, Kang HG, Kim W, Kim WJ, Lee H, Cho JY, Hong R, Kim JW, Chung JY, *et al*: Kindlin-1 promotes gastric cancer cell motility through the Wnt/β-catenin signaling pathway. Sci Rep 15: 2481, 2025.
54. Zhang N, Wei P, Gong A, Chiu WT, Lee HT, Colman H, Huang H, Xue J, Liu M, Wang Y, *et al*: FoxM1 promotes β-catenin nuclear localization and controls Wnt target-gene expression and glioma tumorigenesis. Cancer Cell 20: 427-442, 2011.
55. Dey N, Young B, Abramovitz M, Bouzyk M, Barwick B, De P and Leyland-Jones B: Differential activation of Wnt-β-catenin pathway in triple negative breast cancer increases MMP7 in a PTEN dependent manner. PLoS One 8: e77425, 2013.
56. Zhang YG, Wu S, Lu R, Zhou D, Zhou J, Carmeliet G, Petrof E, Claud EC and Sun J: Tight junction CLDN2 gene is a direct target of the Vitamin D receptor. Sci Rep 5: 10642, 2015.
57. Pereira F, Fernández-Barral A, Larriba MJ, Barbáchano A and González-Sancho JM: From molecular basis to clinical insights: A challenging future for the vitamin D endocrine system in colorectal cancer. FEBS J 291: 2485-2518, 2024.
58. Mariadason JM, Nicholas C, L'Italien KE, Zhuang M, Smartt HJM, Heerdt BG, Yang W, Corner GA, Wilson AJ, Klampfer L, *et al*: Gene expression profiling of intestinal epithelial cell maturation along the crypt-villus axis. Gastroenterology 128: 1081-1088, 2005.